

# Density of states, hybridization, and band-gap evolution in $\text{Al}_x\text{Ga}_{1-x}\text{N}$ alloys

Laurent -C. Duda, Cristian B. Stagarescu,\* James Downes, and Kevin E. Smith<sup>†</sup>

*Department of Physics, Boston University, Boston, Massachusetts 02215*

Dimitris Korakakis and Theodore D. Moustakas

*Department of Electrical and Computer Engineering, Boston University, Boston, Massachusetts 02215*

Jinghua Guo and Joseph Nordgren

*Department of Physics, Uppsala University, Uppsala, Sweden*

(Received 24 December 1997)

The electronic structure of the wurtzite  $\text{Al}_x\text{Ga}_{1-x}\text{N}$  alloy system has been studied for numerous values of Al concentration  $x$  ranging from 0 (pure GaN) to 1 (pure AlN). The occupied and unoccupied partial density of states was measured for each alloy using synchrotron radiation excited soft x-ray absorption and emission spectroscopies. High-resolution x-ray emission spectroscopy allowed the motion of the elementally resolved *bulk* valence-band maximum to be measured as a function of Al concentration. Using this technique we estimate that the value of the band-gap bowing parameter for  $\text{Al}_x\text{Ga}_{1-x}\text{N}$  is zero. Furthermore, the x-ray emission spectra revealed resonantlike emission at approximately 19 eV below the GaN valence-band maximum. By measuring the intensity of this feature as a function of Ga content we prove conclusively that this emission arises from hybridization of N  $2p$  and Ga  $3d$  states. Finally, we find that the N  $K$ - and Al  $K$ -absorption spectra depend strongly on the photon angle of incidence with respect to the surface normal. We explain this in terms of orbital anisotropy in  $\text{Al}_x\text{Ga}_{1-x}\text{N}$ . [S0163-1829(98)03627-3]

## I. INTRODUCTION

The use of GaN, AlN, and  $\text{Al}_x\text{Ga}_{1-x}\text{N}$  alloys in electronic devices has resulted in III-N wide-band-gap semiconductors becoming a very important class of technological materials.<sup>1</sup> The band-gap energies of InN, GaN, and AlN, are 1.9, 3.4, and 6.2 eV, respectively, and in principle optoelectronic devices made from alloys of these materials cover the entire visible to ultraviolet range of the electromagnetic spectrum.<sup>2</sup>  $\text{Al}_x\text{Ga}_{1-x}\text{N}$  alloys have successfully been grown and the band gap found to vary with Al concentration. Nevertheless, there is a significant lack of experimental data concerning the basic electronic structure of these materials. Indeed, to our knowledge the first full band mapping of wurtzite GaN was only recently published,<sup>3</sup> and the intrinsic band structure, the density of states (DOS), and the electronic properties of surfaces are all topics presently under intense scrutiny. While photoemission spectroscopy is a powerful probe of electronic structure in solids that is now being widely applied to III-N semiconductors, it requires that atomically clean surfaces be prepared before bulk properties can be measured.<sup>4-6</sup> The methods for cleaning surfaces of thin-film GaN have been extensively reviewed by Bermudez, and little is known about cleaning  $\text{Al}_x\text{Ga}_{1-x}\text{N}$  surfaces at present.<sup>7</sup> A further problem with photoemission spectroscopy is that, while it does measure band dispersions, it does not measure the partial density of states.<sup>4</sup> (Rather, angle integrated photoemission measures a joint density of states.) The need for complementary probes of electronic structure in these materials is thus clear.

We present here results of a study of the bulk electronic structure of  $\text{Al}_x\text{Ga}_{1-x}\text{N}$  ( $0 \leq x \leq 1$ ) using synchrotron radiation excited soft x-ray emission (SXE) and soft x-ray absorption (SXA) spectroscopies.<sup>8,9</sup> Specifically, we have measured

the elementally resolved partial density of states (PDOS) for a series of  $\text{Al}_x\text{Ga}_{1-x}\text{N}$  alloys. The valence-band contributions of N  $2p$ , and Al  $3p$  states have been measured by recording the  $K$ -edge spectra of N and Al, respectively. We find that the spectra agree well with the corresponding PDOS from an *ab initio* calculation.<sup>10</sup> We also use SXE as a tool to monitor the band-gap variation of  $\text{Al}_x\text{Ga}_{1-x}\text{N}$  alloys as a function of Al content. This allows us to interpolate the band-gap values for all Al concentrations  $x$  and estimate the band-gap bowing parameter  $b$ . We have also used SXE to measure the degree of N  $2p$  hybridization in the shallow Ga  $3d$  core states, and correlate the measured hybridization with Ga content. Finally, we have observed strong angular variations in the SXA spectra that correspond well with predicted orbital anisotropy of the conduction-band states.

## II. EXPERIMENTAL DETAILS

Our samples were thin-film wurtzite  $\text{Al}_x\text{Ga}_{1-x}\text{N}$  ( $0 \leq x \leq 1$ ) grown using electron-cyclotron resonance-assisted molecular-beam epitaxy on sapphire substrates. The samples were  $n$ -type, and the growth procedure has been reported elsewhere.<sup>11</sup> Resistivity, mobility, x-ray diffraction, and photoluminescence studies indicated high-quality films. SXA and SXE measurements were performed at the undulator beam line BW3 at HASYLAB/DESY in Hamburg, Germany, and on undulator beamline X1B at the National Synchrotron Light Source, Brookhaven National Laboratory. Absorption spectra were recorded in the total electron yield mode by measuring the sample drain current and were taken with energy resolutions of approximately 0.1 eV at 400 eV (in the vicinity of the N  $1s$  edge) and 1.5 eV at 1400.0 eV (in the vicinity of the Al  $1s$  edge), corresponding to setting the

monochromator's exit slit width to 80  $\mu\text{m}$ . Since the soft x-ray emission (fluorescence) process is weak compared to the competing nonradiative deexcitation channels, the need for reasonable counting statistics required the use of a larger exit slit width (400  $\mu\text{m}$ , corresponding to an incident photon energy-resolution of about 1 eV) during emission experiments. Emission spectra were recorded using a Nordgren-type grazing-incidence grating spectrometer using a 5-m, 1200-lines/mm grating in first order of diffraction at a resolution of approximately 0.8 eV.<sup>12,13</sup> The acquisition time for individual SXE spectra was approximately 90 min. The base pressure in the experimental system was  $1.0 \times 10^{-8}$  Torr. This vacuum is quite adequate since both SXA and SXE are primarily bulk probes, and surface phenomena were not under investigation. Sample surfaces were not processed or cleaned in the vacuum chamber.

We compare our SXE and SXA spectra of  $\text{Al}_x\text{Ga}_{1-x}\text{N}$  with the *partial* density of states taken from Xu and Ching.<sup>10</sup> The spectra result from the following electronic transitions:  $3p \rightarrow 1s$  (Al  $K$  emission),  $1s \rightarrow 3p$  (Al  $K$  absorption),  $2p \rightarrow 1s$  (N  $K\alpha$  emission), and  $1s \rightarrow 2p$  (N  $K$  absorption). Since the final state in x-ray emission contains a hole in the valence band, one expects that soft x-ray *emission* spectra reflect the ground-state DOS if the final state rule is valid.<sup>14</sup> The final state rule states that the spectral features that appear in x-ray spectroscopy correspond to the theoretical DOS calculated with the final state potential. In general, x-ray *absorption* can only be compared to calculations that take into account *core* hole effects but in favorable cases the resulting distortions are small.<sup>15</sup>

The results of two spectroscopic techniques will be presented, and then compared to theory. While these spectroscopies either measure (SXE) or vary (SXA) a photon energy, it is relative *binding* energies in the materials that are of interest. The procedures used for setting a common binding energy scale are discussed fully in our earlier study of pure GaN.<sup>16</sup> Briefly, we first calibrate our spectrometer detector by using the elastic scattering of incident photons at various energies. The accuracy of this method depends on the combined instrumental resolution of the monochromator and the spectrometer as well as on the relative visibility (number of counts) of the elastic peak. (The monochromator calibration is accurate to within 5%, and since we are using relative energy differences in the spectra, we use the monochromator setting as the photon energy. Clearly the *absolute* energy scale, which is not of primary interest here, is less accurate.) This allows us to plot the SXE spectrum as a function of photon energy, i.e., the emission spectrum is plotted on the same energy scale as the absorption spectrum. For situations where the elastic scattering was too weak to be visible in our spectrometer, we instead record inner-shell transitions and calibrate against known spin-orbit splittings.<sup>16</sup> To put the N emission and absorption spectra on a *binding-energy* scale, we determine the experimental valence-band maximum (VBM) by extrapolating the leading edge of the emission spectrum to zero. Similarly, we adjusted the Al SXE and SXA spectra (separately) so that the Al gap for AlN as derived from theoretical calculations is reproduced. There is thus more uncertainty in the energy scale of the Al spectra than for the N spectra.

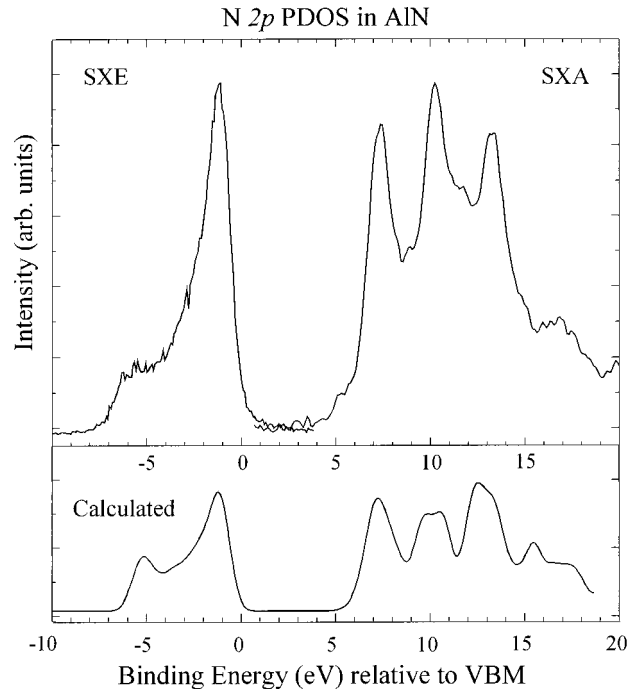


FIG. 1. Comparison of experimental N  $K$ -emission and -absorption spectra from pure AlN (upper panel) with a broadened PDOS from Ref. 10 (lower panel). Note that empty and filled DOS are scaled separately. The energy scale is relative to the experimentally determined valence-band maximum (VBM). See text for details.

### III. RESULTS AND DISCUSSION

#### A. Valence- and conduction-band partial density of states for pure AlN

Figure 1 (top panel) presents the SXE and SXA spectra for N  $2p$  states in pure AlN. Also presented in Fig. 1 (bottom panel) are the results of a first-principles orthogonalized linear-combination of atomic orbitals calculation in the local-density approximation of the N  $2p$  PDOS in AlN.<sup>10</sup> Figure 2 presents equivalent data for the Al  $3p$  states. The theoretical PDOS was first convoluted by Lorentzians to simulate core-hole lifetime broadening and then convoluted by Gaussians to simulate the instrumental broadening. The overall agreement between the measured and calculated PDOS is quite good. SXE and SXA results for pure GaN were presented earlier, and that data also agreed well with N  $2p$  PDOS calculated in the same manner.<sup>16</sup> The absorption spectra shown in Figs. 1 and 2 were taken with the incident photon beam at an angle of incidence of  $45^\circ$ . The experimental occupied bandwidths are found to be somewhat larger than the theoretical ones.<sup>10</sup> Partly, this apparent discrepancy is due to lifetime and instrumental broadening, which are on the order of 0.4 and 0.8 eV, respectively. However, valence-band photoemission spectroscopy also shows a bandwidth much larger than such calculations.<sup>17,18</sup>

#### B. Soft x-ray emission from $\text{Al}_x\text{Ga}_{1-x}\text{N}$ alloys

##### 1. Band-gap evolution

The *occupied* N  $2p$  states of the  $\text{Al}_x\text{Ga}_{1-x}\text{N}$  alloy system was systematically studied by recording N  $K$ -emission spec-

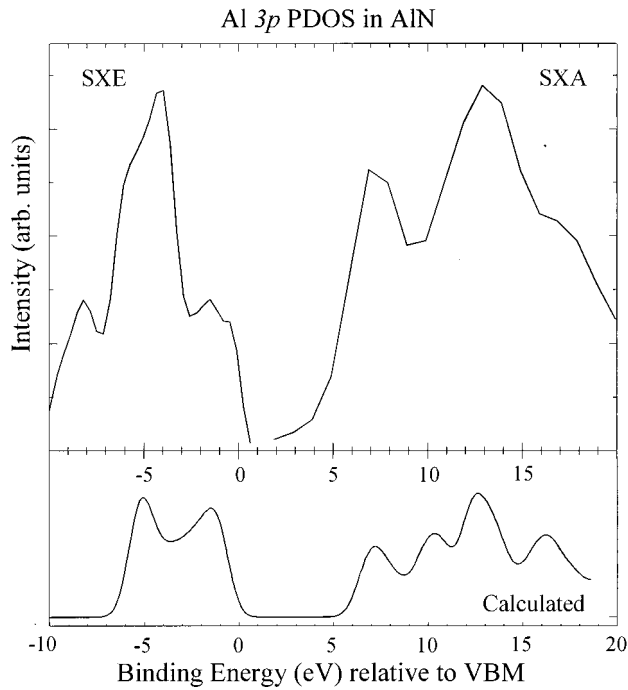


FIG. 2. Similar to Fig. 1, but for Al  $K$  emission and absorption from pure AlN. See text.

tra. Figure 3 presents a series of SXE spectra where the incident photon energy was set above the adsorption edge, nominally at 405 eV. These spectra have not been shifted or aligned in energy in any way, but instead of plotting the spectra relative to the VBM of each alloy, the spectra are each referenced to the AlN VBM as determined from the  $x = 1$  spectrum. A significant narrowing of the  $\text{Al}_x\text{Ga}_{1-x}\text{N}$  valence band with increasing Al concentration is clearly visible. The binding energy of the bottom of the valence band

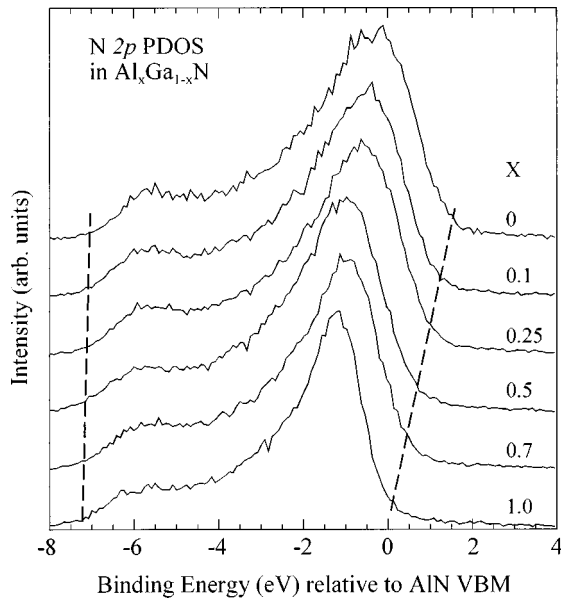


FIG. 3. N  $K$ -emission spectra from  $\text{Al}_x\text{Ga}_{1-x}\text{N}$  ( $0 \leq x \leq 1$ ). Only the valence-band emission is shown. The spectra are not shifted in energy, but plotted relative to the binding energy of the VBM of pure AlN ( $x = 1$ ). The dashed lines indicate the motion of the top and bottom of the valence band, and are guides to the eye.

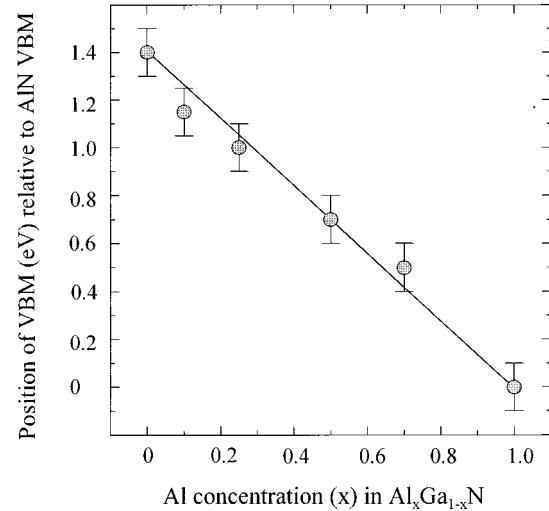


FIG. 4. Data points indicate the position of the experimentally determined VBM for the N  $2p$  PDOS in  $\text{Al}_x\text{Ga}_{1-x}\text{N}$  as a function of  $x$ . The straight line is the predicted position if the bowing parameter  $b$  is zero. See text for details.

remains almost constant, shifting upwards by approximately 0.25 eV, while the top of the valence band moves linearly upwards by 1.4 eV. Technically, it is only the motion of N  $2p$  PDOS that is measured, but since N  $2p$  states dominate the valence band, this is a good measure of the motion of the entire valence band. The experimental behavior of the VBM with Al concentration is plotted in Fig. 4. Theoretically, the behavior of the gap in such an alloy system may be described by the following formula:<sup>19</sup>

$$E_g(x) = \bar{E}_g + \Delta E_g(x - \frac{1}{2}) - bx(1 - x).$$

Here,  $\bar{E}_g$  is the average gap,  $\Delta E_g$  is the difference between the gaps of the pure end members of the alloy system, and  $b$  is the bowing parameter. Early optical studies gave widely variable values of  $b$  ranging from approximately +1.0 eV (Refs. 20 and 21) through  $b = 0$  eV (Ref. 22) to approximately  $b = -0.8$  eV.<sup>23</sup> However, a comprehensive recent optical absorption study of high-quality  $\text{Al}_x\text{Ga}_{1-x}\text{N}$  films found  $b = 0$  eV.<sup>24</sup> Our data indicate that, within experimental error, the VBM varies linearly with  $x$ , and that the band gap opens symmetrically. The former is consistent with a value of  $b = 0$  eV. The latter conclusion comes from the observation that the difference in the bulk band gaps of AlN and GaN is 2.8 eV, and our linear VBM motion is 1.4 eV.

## 2. Hybridization of N $2p$ and Ga $3d$ -states in $\text{Al}_x\text{Ga}_{1-x}\text{N}$

In our recent study of pure GaN we attributed a very weak feature observed at 19 eV below the VBM in the N  $K$  emission to hybridization between N  $2p$  and Ga  $3d$  states.<sup>16</sup> The lack of strict orbital selectivity in photoemission spectroscopy means that such hybrid states cannot be studied using photoemission. By contrast, SXE obeys quite stringent dipole selection rules. Therefore, the N  $K$ -emission spectrum will reflect the  $2p$  states of our nitride samples. Dipole-forbidden  $2s-1s$  transitions are extremely unlikely. However, the poor signal to noise ratio in our original measurement called for a more extensive investigation that could

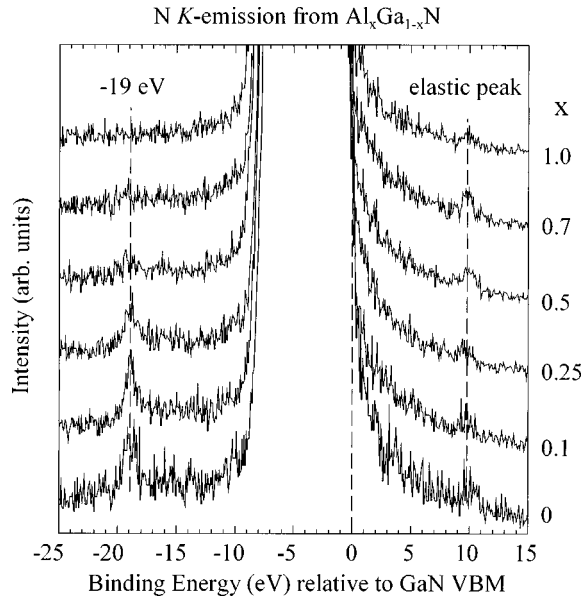


FIG. 5. N  $K$ -emission spectra from  $\text{Al}_x\text{Ga}_{1-x}\text{N}$  ( $0 \leq x \leq 1$ ). This is the same data as in Fig. 3, but the emission above and below the valence band is shown. Note the emission at 19 eV below the GaN VBM. This peak gets weaker and disappears as the Ga content is reduced. It originates from N  $2p$  states hybridized with Ga  $3d$  states.

conclusively identify this emission as being due to hybrid states. The outcome of such a study is of significant interest since it promises that SXE can be widely applied as a probe of hybrid states.

Figure 5 displays the Al-concentration dependence of the hybridization peak that occurs at about 19 eV below the top of the valence band of pure GaN. (Note that here the spectra are plotted relative to the GaN VBM). Within the statistical accuracy of the spectra, no shift of the energy position of this peak with Al concentration is observed. Clearly, the intensity of this feature decreases with decreasing Ga content. Pure AlN (top curve in Fig. 5) has no Ga  $3d$  states, and thus the feature disappears. Moreover, the spectral width of this peak is rather small (resonantlike) whereas the N  $2s$  states of GaN have been shown by photoemission to be quite broad in energy.<sup>25</sup> These findings prove conclusively that this is indeed a hybridization phenomenon and not a signature of dipole-forbidden  $2s$ - $1s$  transitions. Preliminary results from  $\text{In}_x\text{Ga}_{1-x}\text{N}$  alloys that have  $4d$  states at a similar energy to the Ga  $3d$ , indicate that similar hybridization-features are visible.

### C. Angle dependent x-ray absorption spectra of $\text{Al}_x\text{Ga}_{1-x}\text{N}$

When comparing the unoccupied PDOS with absorption measurements, it is important to realize that polarization effects can play an important role. The transition matrix element  $\mathbf{M}$  in the x-ray absorption process contains the scalar product of polarization vector of the incoming photon  $\mathbf{e}$  and the position vector of the electron  $\mathbf{r}$ ,

$$M = \langle \phi_{1s} | \mathbf{e} \cdot \mathbf{r} | \phi_f \rangle,$$

where  $\phi_{1s}$  is the wave function of a N  $1s$  electron and  $\phi_f$  is the wave function of the final state into which the  $1s$  electron

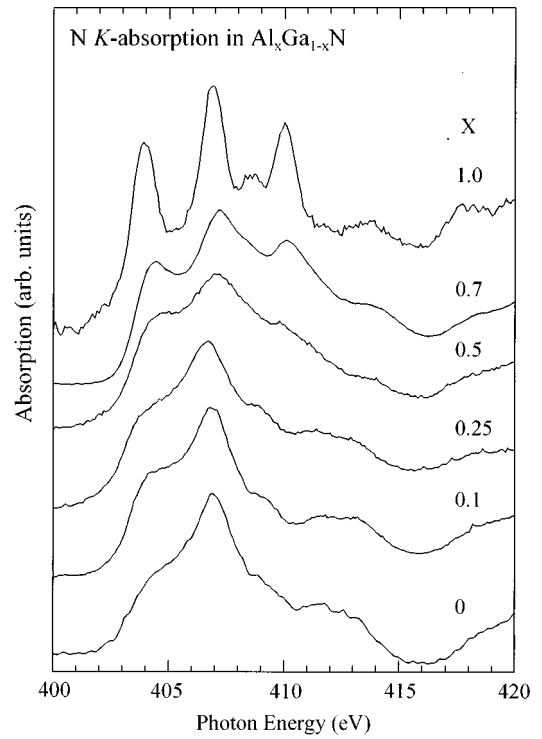


FIG. 6. Unoccupied N PDOS in  $\text{Al}_x\text{Ga}_{1-x}\text{N}$  as measured by SXA (N  $K$  absorption). These spectra are taken in normal incidence mode. Photon energies are as read from the monochromator and are nominal. Spectra have not been energy shifted. See text.

is excited.<sup>9</sup> The dipole transition operator  $\mathbf{e} \cdot \mathbf{r}$  projects out the orbitals along direction of the polarization vector. Thus orbital-symmetry dependent absorption spectra are obtained when using linearly polarized synchrotron radiation. The wurtzite (hexagonal) films under consideration here are grown on basal plane sapphire, and thus the  $\mathbf{c}$  axis coincides with the film normal. Consequently, the  $p_z$  or out-of-plane orbitals are preferentially excited at  $K$  edges when  $\mathbf{e} \perp \mathbf{c}$ . Similarly, the  $p_{x,y}$  or in-plane orbitals are preferentially excited when  $\mathbf{e} \parallel \mathbf{c}$ . Such effects have been reported earlier by Lawniczak-Jablonska *et al.* for N  $K$  absorption in the binary III-nitrides AlN, GaN, and InN.<sup>26</sup>

In Fig. 6 we show angle-dependent N and Al  $K$  absorption spectra for  $\text{Al}_{0.5}\text{Ga}_{0.5}\text{N}$ , pure AlN (Al  $K$ , N  $K$ ), and pure GaN (only N  $K$ ). The SXA spectra clearly exhibit significant variation with angle for all Al concentrations. The solid lines represent the situation of  $\mathbf{e} \perp \mathbf{c}$ , i.e., normal incidence, and the dashed lines represent the approximately situation when  $\mathbf{e} \parallel \mathbf{c}$ , i.e., grazing incidence. In Fig. 7 we present a full series of normal incidence N  $K$ -absorption spectra for the indicated values of  $x$  from 0 to 1. These show that increasing the Al content (bottom to top) leads to sharper spectral features, an indication of an increase in N  $2p$  state localization. This is consistent with the decreased atomic radius in AlN. However, the theoretical DOS from the calculation of Xu and Ching does not reproduce this effect.<sup>10</sup> Note that the onset of the N  $K$  absorption does not change significantly over the entire range of Al concentration. Our SXE data indicate that the band gap opens up symmetrically such that both the valence-band maximum and conduction-band minimum should exhibit the same magnitude shift in energy. Thus a

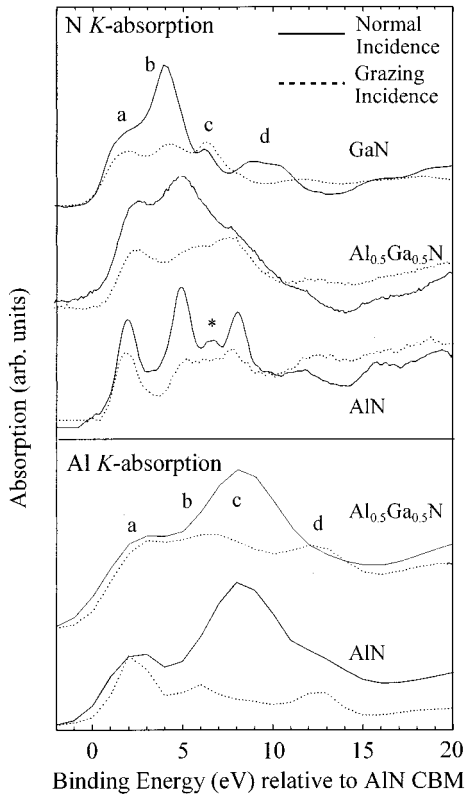


FIG. 7. Polarization effects on SXA spectra in  $\text{Al}_x\text{Ga}_{1-x}\text{N}$ . The top panel shows N  $K$ -absorption spectra for  $x=0, 0.5$ , and  $1.0$ . The bottom panel shows Al  $K$  absorption for  $x=0.5$  and  $1.0$ . Spectra taken with the incident photons in both normal incidence (solid line) and grazing incidence (dashed line) are shown.

shift of 1.4 eV is expected for the onset of the SXA spectra between AlN and GaN. The absence of a shift in the absorption spectra despite the change in the band gap remains to be explained. One possibility is that it is an effect of core-hole distortions of the atomic potential on the final state of the x-ray absorption process. The difference in core-hole screening efficiency due to a change in the band gap can certainly alter the onset energy but this would favor an even larger difference, rather than no change in onset. A further possibility is that this observation is due to core-hole exciton effects. However, in view of the good agreement between the theoretical N  $2p$  PDOS and the x-ray absorption spectra (Fig. 1), this is thought unlikely. A further possibility is that this is due to the chemical shift of the N  $1s$  state binding energy between AlN and GaN.

The orientation dependence in N  $K$  absorption (Fig. 6) for the  $\text{Al}_x\text{Ga}_{1-x}\text{N}$  alloys reveals that the grazing incidence geometry spectra have less pronounced and weaker features than those for normal incidence. This is consistent with the crystal structure, i.e., stronger in-plane and weaker out-of-plane bonding. The spectra were normalized to have equal intensity before the edge and far above the conduction band. Some caution must be taken for effects of saturation that tend to reduce the apparent contrast between background and the genuine spectral features. We note, however, that the behavior of the anisotropy is very similar for all Al concentrations. The main part of the conduction band is about 12–14 eV wide, and we identify four pronounced features

(denoted  $a-d$ ); AlN shows an extra feature (marked with an asterisk in Fig. 6) that appears between  $b$  and  $c$ . The N  $K$ -absorption spectra for GaN and  $\text{Al}_{0.5}\text{Ga}_{0.5}\text{N}$  are very similar in that we find that in-plane character is strongest at energies around 5 eV (feature  $b$ ). The influence of the Al in  $\text{Al}_{0.5}\text{Ga}_{0.5}\text{N}$  is manifested by the small shift to higher energies of the out-of-plane component of feature  $b$ . It is interesting to note that not only the intensity but also the energies of the orbitals vary slightly depending on the angle of incidence of the radiation. This is most evident for feature  $b$  in  $\text{Al}_{0.5}\text{Ga}_{0.5}\text{N}$  and AlN where the out-of-plane orbital has a slightly higher energy than its in-plane counterpart.

The Al  $K$ -absorption spectra for  $\text{Al}_{0.5}\text{Ga}_{0.5}\text{N}$  and AlN in Fig. 6 were taken at much lower resolution, approximately 1.5 eV. The spectra are quite similar to each other, indicating little interaction between Ga and Al sites in the alloys. The dependence of the Al  $K$ -absorption spectra on the polarization of the incident radiation is much stronger than for the N  $K$ -absorption spectra, especially above 4 eV. The corresponding antibonding orbitals have almost purely in-plane orientation. Feature  $c$  at about 9 eV is dominant in the normal incidence spectrum but has completely vanished in the grazing incidence spectrum where  $\mathbf{e} \parallel \mathbf{c}$ .

#### IV. SUMMARY AND CONCLUSIONS

We have studied the electronic structure of the  $\text{Al}_x\text{Ga}_{1-x}\text{N}$  alloy system using soft x-ray absorption and emission spectroscopy. We interpret both types of spectra in terms of the partial density of states. Comparison to an *ab initio* calculation shows good agreement. The narrowing of the valence band with increasing Al content is found to take place almost entirely at the top of the valence band, with the bottom of the valence band remaining essentially fixed. The spectral features and the width of the N  $K$ - and Al  $K$ -absorption spectra show good correspondence to the structures in the unoccupied PDOS. However, we find that there is strong anisotropy in the unoccupied N  $2p$  and Al  $2p$  states that need to be taken into account when comparing to the PDOS. The effect of the change in the band gap with varying Al content was observed in N  $K$ -emission spectra. We estimate from these spectra that the bowing parameter  $b$  for  $\text{Al}_x\text{Ga}_{1-x}\text{N}$  is zero. Finally, a sharp emission feature at 19 eV below the GaN valence-band maximum was proved to originate from N  $2p$  states hybridizing resonantly with Ga  $3d$  states.

#### ACKNOWLEDGMENTS

This work was supported in part by the National Science Foundation under Grant No. DMR-9504948. Our x-ray emission spectrometer is funded by the U.S. Army Research Office under Grant No. DAAH04-95-0014. Some experiments were performed at the NSLS, which is supported by the U.S. Department of Energy, Divisions of Materials and Chemical Sciences. The Uppsala program was supported in part by the Swedish Natural Research Council (NFR) and the Göran Gustafsson Foundation. We are also indebted to HASYLAB/DESY staff for valuable technical support. T.D.M. acknowledges the support of DoD/ARPA under Grant No. MDA972-96-3-0014. L.-C.D. gratefully acknowledges a grant from NFR.

- \*On leave from the Institute of Microtechnology, Bucharest, Romania.
- †Author to whom correspondence should be addressed. Electronic address: ksmith@bu.edu
- <sup>1</sup>M. Misra *et al.*, in *III-V Nitrides*, edited by F. A. Ponce, T. D. Moustakas, I. Akasaki, and B. A. Monema (Materials Research Society, Pittsburgh, 1996), Vol. 449, p. 597.
  - <sup>2</sup>S. Strite and H. Morkoç, *J. Vac. Sci. Technol. B* **10**, 1237 (1992).
  - <sup>3</sup>S. S. Dhesi, C. B. Stagaescu, K. E. Smith, D. Doppalapudi, R. Singh, and T. D. Moustakas, *Phys. Rev. B* **56**, 10 271 (1997).
  - <sup>4</sup>*Photoemission in Solids, Parts 1 and 2*, edited by M. Cardona and L. Ley (Springer-Verlag, Berlin, 1978).
  - <sup>5</sup>*Angle Resolved Photoemission*, edited by S. D. Kevan (Elsevier, Amsterdam, 1991).
  - <sup>6</sup>K. E. Smith and S. D. Kevan, *Prog. Solid State Chem.* **21**, 49 (1991).
  - <sup>7</sup>V. M. Bermudez, *Appl. Surf. Sci.* (to be published).
  - <sup>8</sup>L. G. Paratt, *Rev. Mod. Phys.* **31**, 616 (1959).
  - <sup>9</sup>J. Stöhr, *NEXAFS Spectroscopy* (Springer, Berlin, 1992).
  - <sup>10</sup>Y.-N. Xu and W. Y. Ching, *Phys. Rev. B* **48**, 4335 (1993).
  - <sup>11</sup>T. Lei, M. Fanciulli, R. J. Molnar, T. D. Moustakas, R. J. Graham, and J. Scanlon, *Appl. Phys. Lett.* **59**, 944 (1991).
  - <sup>12</sup>J. Nordgren, G. Bray, S. Cramm, R. Nyholm, J.-E. Rubensson, and N. Wassdahl, *Rev. Sci. Instrum.* **60**, 1690 (1989).
  - <sup>13</sup>J. Nordgren and R. Nyholm, *Nucl. Instrum. Methods Phys. Res. A* **246**, 242 (1986).
  - <sup>14</sup>U. v. Barth and G. Grossmann, *Phys. Rev. B* **25**, 5150 (1982).
  - <sup>15</sup>F. M. F. d. Groot, *J. Electron Spectrosc. Relat. Phenom.* **67**, 529 (1994).
  - <sup>16</sup>C. B. Stagaescu, L.-C. Duda, K. E. Smith, J. H. Guo, J. Nordgren, R. Singh, and T. D. Moustakas, *Phys. Rev. B* **54**, 17 335 (1996).
  - <sup>17</sup>G. Martin, S. Strite, A. Botchkarev, A. Agarwal, A. Rockett, W. R. L. Lambrecht, B. Segall, and H. Morkoc, *J. Electron. Mater.* **24**, 225 (1995).
  - <sup>18</sup>G. Martin, S. Strite, A. Botchkarev, A. Agarwal, A. Rockett, H. Morkoc, W. R. L. Lambrecht, and B. Segall, *Appl. Phys. Lett.* **65**, 610 (1994).
  - <sup>19</sup>E. A. Albanesi, W. R. L. Lambrecht, and B. Segall, *Phys. Rev. B* **48**, 17 841 (1993).
  - <sup>20</sup>M. R. H. Khan, Y. Koide, H. Itoh, N. Sawaki, and I. Akasaki, *Solid State Commun.* **60**, 509 (1986).
  - <sup>21</sup>Y. Koide, H. Itoh, M. R. H. Khan, K. Hiramatsu, N. Sawaki, and I. Akasaki, *J. Appl. Phys.* **61**, 4540 (1987).
  - <sup>22</sup>M. A. Kahn, R. A. Skogman, R. G. Schulze, and M. Gershenzon, *Appl. Phys. Lett.* **43**, 492 (1983).
  - <sup>23</sup>S. Yoshida, S. Misawa, and S. Gonda, *J. Appl. Phys.* **53**, 6844 (1982).
  - <sup>24</sup>D. K. Wickenden, C. B. Barger, W. A. Bryden, J. Miragliotta, and T. J. Kistenmacher, *Appl. Phys. Lett.* **65**, 2024 (1994).
  - <sup>25</sup>S. A. Ding, G. Neuhold, J. H. Weaver, P. Haberle, K. Horn, O. Brandt, H. Yang, and K. Ploog, *J. Vac. Sci. Technol. A* **14**, 819 (1996).
  - <sup>26</sup>K. Lawniczak-Jablonska, T. Suski, Z. Liliental-Weber, E. M. Gullikson, J. H. Underwood, R. C. C. Perera, and T. J. Drummond, *Appl. Phys. Lett.* **70**, 2711 (1997).